

# Fast Radio Bursts from White Dwarf Binary Mergers: Isolated and Triple-Induced Channels

CHEYANNE SHARIAT,<sup>1</sup> CLAIRE S. YE,<sup>2</sup> SMADAR NAOZ,<sup>3,4</sup> AND SANAEA ROSE<sup>5</sup>

<sup>1</sup>*Department of Astronomy, California Institute of Technology, 1200 East California Boulevard, Pasadena, CA 91125, USA*

<sup>2</sup>*Canadian Institute for Theoretical Astrophysics, University of Toronto, 60 St George Street, Toronto, ON M5S 3H8, Canada*

<sup>3</sup>*Department of Physics and Astronomy, University of California, Los Angeles, CA 90095, USA*

<sup>4</sup>*Mani L. Bhaumik Institute for Theoretical Physics, Department of Physics and Astronomy, UCLA, Los Angeles, CA 90095, USA*

<sup>5</sup>*Center for Interdisciplinary Exploration and Research in Astrophysics (CIERA), Northwestern University, 1800 Sherman Ave, Evanston, IL 60201, USA*

## ABSTRACT

The detection of fast radio bursts (FRBs) in both young and old stellar populations suggests multiple formation pathways, beyond just young magnetars from core-collapse supernovae. A promising delayed channel involves the formation of FRB-emitting neutron stars through merger- or accretion-induced collapse of a massive white dwarf (WD). By simulating a realistic stellar population with both binaries and triples, we identify pathways to WD collapse that could produce FRB candidates. We find that (i) triple dynamics open new merger channels inaccessible to isolated binaries, significantly enhancing the overall merger rate; (ii) triple-induced mergers broaden the delay-time distribution, producing long-delay ( $\gtrsim 1\text{--}8$  Gyr) events largely independent of metallicity, alongside a shorter-delay population ( $\lesssim 100$  Myr) of rapid mergers; (iii) these long delays naturally yield FRBs in older environments such as quiescent host galaxies and galactic halos; (iv) when convolved with the cosmic star-formation history, binary channels track the star-formation rate ( $z_{\text{peak}} \sim 2$ ), while triple channels peak later ( $z_{\text{peak}} \sim 1$ ), giving a combined local source rate of  $R_0 \approx 2 \times 10^4 \text{ Gpc}^{-3} \text{ yr}^{-1}$ , consistent with observations; and (v) applying the same framework to Type Ia supernovae, we find that triples extend the delay-time tail and roughly double the Ia efficiency relative to binaries, yielding rates and redshift evolution in good agreement with observations. If FRBs originate from the collapse of WDs, our results establish triples, alongside binaries, as a crucial and previously overlooked formation pathway whose predicted rates, host demographics, and redshift evolution offer clear tests for upcoming surveys.

## 1. INTRODUCTION

Fast radio bursts (FRBs) are millisecond-duration radio transients with dispersion measures (DMs) often exceeding the Galactic contribution, implying extragalactic and even cosmological distances (Lorimer et al. 2007; Thornton et al. 2013; Petroff et al. 2019; CHIME/FRB Collaboration et al. 2020). Despite their high event rates ( $\sim 10^3\text{--}10^4 \text{ sky}^{-1} \text{ day}^{-1}$ ; Bhandari et al. 2018; Ravi 2019; CHIME/FRB Collaboration et al. 2021), the nature of FRBs remains unresolved. The detection of a fast radio burst from the Galactic magnetar SGR 1935+2154 (CHIME/FRB Collaboration et al. 2020; Bochenek et al. 2020) has established magnetars as a leading channel. However, FRBs exhibit a wide diversity in phenomenology, such as repeating and apparently non-repeating bursts, polarization properties, and host galaxy demographics (e.g., Bannister et al. 2019;

Prochaska et al. 2019; Heintz et al. 2020; Bhandari et al. 2020; Petroff et al. 2022; Gordon et al. 2025; Horowicz & Margalit 2025). These diverse properties strongly suggest that multiple progenitor pathways contribute to FRBs.

FRB progenitor models are often divided into two broad classes: *prompt* and *delayed*. In *prompt* channels, FRBs are powered by compact objects formed shortly after a star formation episode ( $\lesssim 100$  Myr), such as young magnetars born in core-collapse supernovae (e.g., Metzger et al. 2017; CHIME/FRB Collaboration et al. 2020; Bochenek et al. 2020). In *delayed* channels, the FRB engine forms on longer timescales ( $\gtrsim 0.1\text{--}1$  Gyr) through binary interactions, including accretion-induced collapse (AIC) of massive white dwarfs (WDs), compact object mergers, or other accretion-powered pathways (Totani 2013; Kashiyama et al. 2013; Wang et al. 2016; Deng et al. 2021; Sridhar et al. 2021; Rao et al. 2025). Host galaxy studies support the presence of both prompt and delayed channels: a majority of FRBs are found in star-forming galaxies (e.g., Bassa et al. 2017;

Marcote et al. 2017; Margalit & Metzger 2018; Marcote et al. 2020; Bhardwaj et al. 2021a; Niu et al. 2022; Michilli et al. 2023; Sharma et al. 2024; Bruni et al. 2024, 2025; Gordon et al. 2025; Horowicz & Margalit 2025), while another fraction reside in the outskirts of galaxies or quiescent elliptical galaxies (e.g., Chatterjee et al. 2017; Marcote et al. 2017; Tendulkar et al. 2017; Fong et al. 2021; Bhardwaj et al. 2021b; Bhandari et al. 2022; Kirsten et al. 2022; Ravi et al. 2022; Michilli et al. 2023; Sharma et al. 2023; Shah et al. 2025; Gordon et al. 2025; Horowicz & Margalit 2025). Notably, the association of an FRB source with a globular cluster in M81 (Bhardwaj et al. 2021b; Kirsten et al. 2022) demonstrates that strongly magnetized neutron stars, the likely central engines of FRBs, can form not only from the core collapse of young massive stars, but also from the merger-induced collapse or AIC of old WDs (Kremer et al. 2021; Lu et al. 2022; Rao et al. 2025).

A promising way to distinguish between these scenarios is through the redshift evolution of the volumetric FRB rate (e.g., James et al. 2022; Zhang et al. 2024; Meng & Deng 2025). However, current constraints remain weak due to ambiguity between DM and redshift, complex selection biases, and the difficulty in disentangling repeating from non-repeating sources. (e.g., Hashimoto et al. 2022; Shin et al. 2023; Lei et al. 2025).

Among delayed channels, mergers involving massive WDs are particularly compelling. Both single-degenerate and double-degenerate pathways have been proposed to produce highly magnetized WDs (e.g., Dessart et al. 2007; Kashiyama et al. 2013) or trigger AIC into magnetized neutron stars capable of powering FRBs (e.g., Nomoto & Kondo 1991; Usov 1992; Shen et al. 2012; Margalit et al. 2019; Schwab 2021; Combi et al. 2025). Previous studies have explored binary WD mergers as FRB progenitors (e.g., Kashiyama et al. 2013; Lu et al. 2022; Kremer et al. 2021, 2023; Rao et al. 2025), and Cao et al. (2018) showed that their predicted rates are among the most consistent with observed FRB statistics.

However, a large fraction of the stars that evolve into massive WDs ( $M_{\text{WD}} \gtrsim 0.8 M_{\odot}$ ), the likely progenitors of magnetized compact objects, originate in hierarchical triple systems. This makes triples a natural and potentially dominant environment for forming FRB progenitors. On the main sequence,  $\sim 35\%$  of  $\sim 2 M_{\odot}$  stars and nearly  $\sim 50\%$  of  $\sim 8 M_{\odot}$  stars reside in triple star systems (Raghavan et al. 2010; Tokovinin 2014a; Moe & Di Stefano 2017; Moe & Kratter 2021; Shariat et al. 2025a; Offner et al. 2023). Among triples in the Galactic field, effectively all are observed to be hierarchical (e.g., Tokovinin 2014b, 2022; Shariat et al. 2025a),

where an inner binary resides on a relatively tighter inner orbit compared to the more distant tertiary star. In this configuration, the outer binary is defined between the tertiary star and the inner binary's center of mass. In such hierarchical triples, secular gravitational interactions between the inner and outer orbit give rise to the eccentric Kozai-Lidov (EKL) mechanism (Kozai 1962; Lidov 1962; Naoz 2016), whereby the inner binary experiences eccentricity-inclination oscillations. EKL oscillations can excite large eccentricities in the inner binary, decreasing its periastron distances, which in turn can lead to tidal circularization, mass transfer, and/or a stellar merger. As a result, triples provide new evolutionary pathways to inner binaries that are inaccessible to isolated binaries. Prior studies have shown that triple dynamics are critical for the formation of accreting WD binaries (Knigge et al. 2022; Shariat et al. 2025b), ultracompact WD binaries (e.g., Toonen et al. 2016, 2020; Shariat et al. 2023, 2025d; Rajamuthukumar et al. 2025), X-ray binaries (e.g., Naoz et al. 2016; Shariat et al. 2025c; Xuan et al. 2025), and compact object mergers including neutron stars and black holes (e.g., Antonini et al. 2014; Thompson 2011a; Shappee & Thompson 2013; Toonen et al. 2018; Fragione & Loeb 2019a,b; Stegmann et al. 2022; Stegmann & Klencki 2025; Perets 2025). These findings cement triples as a necessary component for modeling compact object formation and evolution.

In this *Letter*, we present the first systematic study of FRB candidates formed from WD mergers in a stellar population including both isolated binaries and hierarchical triples<sup>1</sup>. We compare the population demographics of triples – such as delay time distributions and source rates – to isolated binary simulations to predict their respective roles in the formation of FRB candidates. The remainder of this study is organized as follows: Section 2 outlines the methodology, including the setup of our binary and triple simulations. In Section 3 we highlight the key results, including the triple formation pathways (Section 3.1), delay time distributions (Section 3.2), and redshift evolution (Section 3.3). Lastly, we summarize the main conclusions in Section 4. A discussion on Type Ia supernovae and supplementary tables is provided in Appendix A.

## 2. METHODOLOGY

### 2.1. Triple Population and Initial Conditions

<sup>1</sup> see also Decoene et al. (2021), who discuss accreting surrounding debris into a central compact object to power FRB emission through EKL dynamics

Throughout this paper, we consider hierarchical triple star systems with two stars in the inner binary (masses  $m_1, m_2$ ) and a more distant third (tertiary) star (mass  $m_3$ ) on an outer orbit. The inner (outer) binary has a semi-major axis, period, eccentricity, and mass ratio of  $a_{\text{in}}$  ( $a_{\text{out}}$ ),  $P_{\text{in}}$  ( $P_{\text{out}}$ ),  $e_{\text{in}}$  ( $e_{\text{out}}$ ), and  $q_{\text{in}} = m_2/m_1$  ( $q_{\text{out}} = m_3/(m_1 + m_2)$ ). The inner binary mass ratio is defined as  $q_{\text{in}} = m_1/m_2$ , where  $m_1$  is the *initially* more massive star. The mutual inclination of the two orbits is given by  $i_{\text{mut}}$ .

We adopt realistic initial conditions for our stellar triple populations based on the empirical distributions derived by [Shariat et al. \(2025a\)](#), which are anchored in *Gaia* observations. In brief, the inner binary properties ( $M_1, q_{\text{in}}, P_{\text{in}}, e_{\text{in}}$ ) are drawn covariantly from the distributions of [Moe & Di Stefano \(2017\)](#). The outer orbit follows a log-normal period distribution, thermal eccentricity distribution, and a  $q_{\text{out}}$  drawn from a power law with slope  $-1.4$ . Mutual inclinations are assumed isotropic, and all triples are made hierarchical and dynamically stable. Specifically, we require both the octupole hierarchical criterion ([Naoz et al. 2013a](#))

$$\epsilon = \frac{a_1}{a_2} \frac{e_2}{1 - e_2^2} < 0.1, \quad (1)$$

and the stability criterion ([Mardling & Aarseth 2001](#)):

$$\frac{a_2}{a_1} > 2.8 \left( 1 + \frac{m_3}{m_1 + m_2} \right)^{2/5} \frac{(1 + e_2)^{2/5}}{(1 - e_2)^{6/5}} \quad (2)$$

are satisfied. All of the above are consistent with the resolved triple population, as observed by *Gaia* ([Shariat et al. 2025a](#)). Moreover, the sampling results in multiplicity fractions, i.e., relative fractions of singles, binaries, and triples, that are consistent with current observations ([Moe & Di Stefano 2017](#); [Offner et al. 2023](#); [Shariat et al. 2025a](#)).

## 2.2. Secular Evolution and Stellar Interactions

For each triple, we solve the hierarchical, secular three-body equations of motion up to the octupole level<sup>2</sup> of approximation (see [Naoz 2016](#)), including the 1st Post Newtonian term for general relativity precession ([Ford et al. 2000](#); [Naoz et al. 2013b](#)). Tidal evolution is mod-

<sup>2</sup> We neglect the hexadecapole ( $(a_1/a_2)^5$ ; [Will 2017, 2021](#); [Conway & Will 2024](#)) and higher-order terms. Although such corrections can be important in some regimes (e.g., [Holzknecht et al. 2025](#); [Naoz et al. 2025](#)), they are expected to be subdominant here, given the wide outer orbits and typically unequal component masses of our systems.

eled using the equilibrium tides<sup>3</sup> formalism ([Hut 1980](#); [Eggleton et al. 1998](#)), with different prescriptions for convective and radiative envelopes based on the stellar type ([Zahn 1977](#); [Stephan et al. 2016](#)).

Single stellar evolution is included for all three stars in the triple using **SSE** ([Hurley et al. 2000](#)). The long-term evolution was tested in previous studies (e.g., [Naoz et al. 2016](#); [Stephan et al. 2016](#); [Angelo et al. 2022](#); [Shariat et al. 2023, 2025d](#)). Binaries that begin mass transfer are removed from the triple evolution and are then followed using the **COSMIC** binary evolution code ([Breivik et al. 2020](#)), which also uses **SSE** prescription ([Hurley et al. 2002](#)). Since short-range processes such as tides and mass transfer operate on timescales much shorter than the secular perturbations from the tertiary, the subsequent evolution can be accurately treated using isolated binary evolution. The settings used in **COSMIC** are set to the defaults, with the following changes: `qcflag` = 4, `don_lim` = -2. `qcflag` determines the critical mass ratio for unstable mass transfer during Roche Lobe overflow, where setting `qcflag` = 4 follows the prescription of [Belczynski et al. \(2008\)](#), except for WD donors, which follow [Hurley et al. \(2002\)](#). Setting `don_lim` = -2 assumes a donor mass loss rate following [Claeys et al. \(2014\)](#).

Each system is evolved for a random time chosen from  $\mathcal{U}(0, 12.5)$  Gyr to model a constant star formation history, representative of the local Milky Way population. Note that this choice is mostly inconsequential to our rate estimations since we focus mainly on the delay times: the time it takes to form an FRB candidate after the system forms. We also re-run the same population assuming three different metallicities:  $Z_{\odot}$ ,  $0.1 Z_{\odot}$ , and  $0.01 Z_{\odot}$ .

## 2.3. Binary Population

In addition to our triple simulations, we evolve a control population of isolated binaries using **COSMIC**. For this comparison, the inner binaries from our triple sample are re-initialized as stand-alone binaries, evolved with identical stellar evolution prescriptions, and for the same evolution time. This parallel binary population serves two purposes. First, it provides a baseline for

<sup>3</sup> Note that here we adopt the equilibrium tide for both stars and WDs. They often tend to underestimate the efficiency of the tides compared to chaotic dynamical tides for sufficiently large eccentricity (e.g., [Vick et al. 2019](#)). Further, considering tight WD+WD binaries, dynamical tides also play an important role in the final stages of circularization and shrinking (e.g., [Fuller & Lai 2012](#); [Vick et al. 2017](#); [Su & Lai 2022](#); [Xuan et al. 2025](#)). Nonetheless, because the main driver of the dynamics takes place during the point-mass stage, we expect that the details of the tides would not qualitatively alter the results.

assessing how binary evolution alone contributes to potential FRB progenitors. Second, it allows us to isolate the role of secular three-body dynamics in modifying merger pathways. By evolving both populations consistently, we can directly quantify the unique characteristics of triple dynamics relative to isolated binary evolution on the predicted FRB candidate rate and delay time distribution.

#### 2.4. FRB Candidate Identification

The physical origin of FRBs remains uncertain. Their inferred all-sky rates suggest that they are produced by a common class of astrophysical events (e.g., Petroff et al. 2019; Ravi et al. 2022), yet proposed progenitors span a wide range, from magnetars to various classes of compact object mergers (e.g., Kashiyama et al. 2013; Totani 2013; Wang et al. 2016; Platts et al. 2019). In this work, we adopt an agnostic approach and explore several merger pathways involving WDs that may lead to FRB production. Specifically, our models include three potential FRB formation pathways and one alternative outcome (SNe Ia):

1. **FRB Candidate –  $O/Ne+Any$ :** merger- or accretion-induced collapse of an O/Ne WD with any companion type (degenerate or non-degenerate).
2. **FRB Candidate –  $WD+WD$ :** merger between two carbon-oxygen (CO) WDs of any mass.
3. **FRB Candidate – massive  $WD+WD$ :** mergers between a massive white dwarf ( $M > 0.85 M_{\odot}$ ), either O/Ne or CO, and another CO white dwarf.
4. **SNe Ia Candidates – massive  $WD$  mergers:** We adopt two criteria for SNe Ia progenitors: (i) mergers between a massive CO WD ( $> 0.85 M_{\odot}$ ) and WD, including CO and He WDs<sup>4</sup>, and (ii) mergers between two CO WDs of any mass. We note that FRB candidates are of interest here; see Appendix A for details on SNe Ia rates from our models.

The first channel ( $O/Ne+Any$ ) corresponds exclusively to super-Chandrasekhar accretion- or merger-induced collapse of O/Ne white dwarfs. This channel is motivated by models in which the collapse of an O/Ne WD produces a rapidly rotating, highly magnetized neutron star that is a plausible FRB engine (e.g., Nomoto

& Kondo 1991; Usov 1992; Schwab 2021; Combi et al. 2025).

The two WD+WD channels (Cases 2 and 3) allow us to explore double-white dwarf mergers more generally. Although CO+CO mergers are often associated with Type Ia supernovae, a fraction may instead avoid thermonuclear explosion and produce either a massive, strongly magnetized WD or undergo collapse into a neutron star: both discussed as potential FRB progenitors (García-Berro et al. 2012; Kashiyama et al. 2013; Schwab 2021). Observationally, magnetic WDs are systematically heavier than their non-magnetic counterparts (e.g., Liebert et al. 2003; Tout et al. 2008; Kawka et al. 2007; García-Berro et al. 2012; Kepler et al. 2013; Caiazzo et al. 2021; Jewett et al. 2024), supporting the idea that they originate from mergers.

For these reasons, we do not impose a Chandrasekhar-mass requirement on WD+WD mergers in our FRB channels. Nonetheless, the majority of our systems are near-Chandrasekhar: approximately 70% of Case 2 mergers and 100% of Case 3 mergers have total mass exceeding  $1.35 M_{\odot}$ .

We emphasize that we make no assumption that these mergers necessarily produce FRBs. Instead, we treat them as candidate pathways to quantify their intrinsic rates and delay-time distributions, and compare the results between triples and isolated binaries. By following the full evolutionary tracks and tagging outcomes such as CO+CO, O/Ne+CO, or O/Ne+non-degenerate mergers, we identify the stellar pathways that could, in principle, give rise to FRBs without presuming the mechanism that ultimately powers the bursts.

## 3. RESULTS

### 3.1. Formation Channels of FRBs in Triples

After evolving the triple population, we track those that become one of the aforementioned FRB progenitor candidates<sup>5</sup>. Figure 1 illustrates the formation pathways of FRBs in triple star systems, as observed in our simulated population. An initial inner binary at the zero-age main sequence (ZAMS,  $t = 0$ ) is split into three main evolutionary branches based on when mass transfer first begins. The parenthesized fractions indicate their percentage contribution relative to the entire simulated FRB candidate population.

1. **eccentric  $RG+MS$  (93%):** The most common scenario is that mass transfer first initiates in the inner binary when the primary evolves to become a

<sup>4</sup> Note that He WDs are excluded from our FRB analysis because it is unclear whether they can cause WD collapse or a detonation on the primary WD’s surface (e.g., Shen et al. 2012; Shen & Bildsten 2014; Shen & Moore 2014; Shen 2025).

<sup>5</sup> Note that the full set of outcomes from this evolution is discussed in greater detail in Shariat et al. in prep.

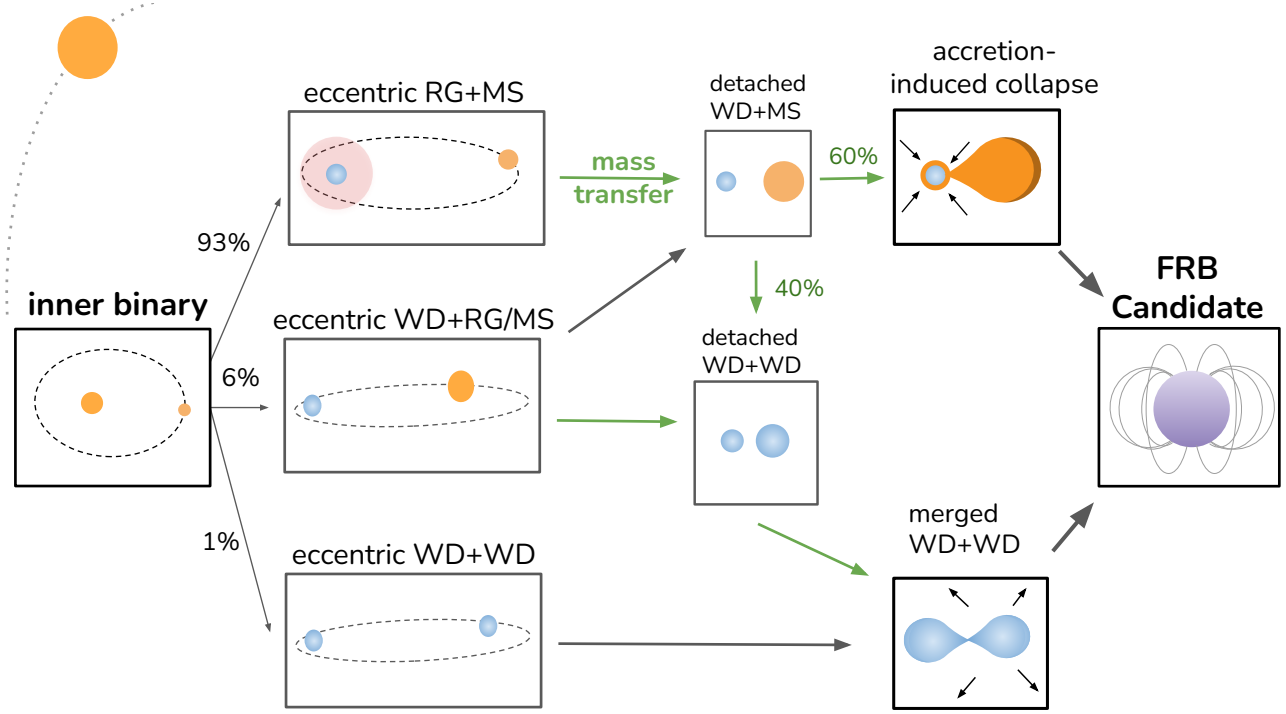


**Figure 1.** Possible formation pathways of FRB candidates in triple star systems. Stages of mass transfer (MT), either dynamically stable or unstable, are denoted with green arrows. On the left, we first start with a triple star system containing three main-sequence stars. The first stage of MT in the inner binary can occur when it is an RG+MS, WD+MS/RG, or WD+WD. The evolution follows until the merger of two WDs (35% of FRB progenitors) or AIC of a white dwarf in a single degenerate scenario (65%). Note that these pathways only represent systems that will become FRB candidates. Broader triple outcomes and their relative fractions are described in Shariat et al. (in prep).

red giant<sup>6</sup> (RG). The RG+MS mass transfer can either be stable or unstable, the latter of which leads to a common envelope stage. If the binary does not merge, the result of mass transfer will be a detached WD+MS binary, which can undergo another phase of mass transfer, either stable or unstable. During stable mass transfer, the system would be a cataclysmic variable (CV), at which point it could potentially undergo AIC, making it an FRB candidate. Otherwise, both stable or unstable WD+MS mass transfer could result in a tight, detached WD+WD binary, which could merge and become an FRB candidate.

2. *eccentric WD+RG/MS* (6%): The second most common outcome is when mass transfer first occurs between a WD+MS or WD+RG inner binary. In this case, the WD evolved independently in an initially wide inner binary ( $\gtrsim 10$  au), producing a wide detached WD+MS inner binary. Extreme ec-

centricities caused by EKL dynamics led to a small periastron separation, allowing tides to shrink and circularize the orbit. Later on, a phase of WD+MS mass transfer begins, resulting in either AIC if the WD retains enough mass to surpass the Chandrasekhar limit or a close WD+WD binary that eventually merges due to gravitational waves, both of which make them FRB candidates.

3. *eccentric WD+WD* ( $\sim 1\%$ ): This channel involves head-on collisions of wide WD+WD binaries driven to extreme eccentricities by octupole-level EKL oscillations. In these systems, an initially wide inner binary ( $a_{\text{in}} \gtrsim 10$  au) reaches  $e_{\text{in}} \gtrsim 0.999$ , reducing the periastron to  $\lesssim 10^{-2}$  au and triggering a direct collision. Although eccentric WD+WD mergers represent only a small fraction ( $\sim 1\%$ ) of the overall merger population, they contribute significantly by extending the delay times of WD+WD mergers in the overall population (often several Gyr; Section 3.2). This channel is therefore an important contributor to the long-delay merger population in FRBs, and has

<sup>6</sup> We use the class ‘red giant’ liberally to encompass various post-main sequence stars including subgiants, red giants, and AGB stars.

**Table 1.** Fractions of triple and binary stellar systems that evolve into each progenitor channel at solar metallicity.

Channel	Triple	Binary
<i>O/Ne WD+any</i>	$1.9 \times 10^{-3}$	$1.4 \times 10^{-3}$
<i>WD+WD</i>	$4.3 \times 10^{-3}$	$3.2 \times 10^{-3}$
<i>massive WD+WD</i>	$2.3 \times 10^{-3}$	$1.6 \times 10^{-3}$

also been studied in the context of Type Ia supernovae (e.g., Toonen et al. 2018).

The excitation of eccentricity via EKL, followed by tidal migration also delays the onset of Roche-lobe overflow in many RG+MS systems until the red giant is more evolved. In such cases, mass transfer begins at wider orbital separations with greater orbital energy, which can sometimes stabilize otherwise unstable interactions and allow the binary to survive. This mechanism, therefore, not only alters the stability of mass transfer but also extends the delay time for FRB candidate formation relative to isolated binaries.

Compared to isolated binaries, mass-transfer interactions between RG+MS or WD+RG/MS systems occur more frequently in triples. This enhancement arises because wide inner binaries in hierarchical triples unavoidably undergo eccentricity oscillations via the EKL mechanism, which can shrink their periastron distances over time. As a result, binaries that would have otherwise remained detached can experience Roche-lobe overflow, either before or after one component evolves into a WD. In RG+MS systems, this process delays the onset of Roche-lobe overflow until the RG is more evolved or is even on the asymptotic giant branch (AGB). Starting mass transfer later and at typically wider orbital separations aids in surviving common envelope evolution, which increases the rate of FRB candidates in triples and extends their delay times relative to isolated binaries (Table 1).

Note that some WD mergers could also lead to SNe Ia supernovae. Specifically, mergers involving He WDs (not considered in any of our FRB channels) and/or CO WDs with a massive CO primary ( $\gtrsim 0.9 M_{\odot}$ ) are among the most promising Type Ia candidates (e.g., Guilluchon et al. 2010; Ruiter et al. 2011; Shen et al. 2018, 2021; Shen 2025). While spatial coincidence between FRBs and Type Ia supernovae could support the idea of WD mergers as FRB progenitors (e.g., Kashiyama et al. 2013), the most plausible progenitor class con-

sidered here involves O/Ne WDs, which are unlikely to produce SNe Ia. Nonetheless, the same triple-induced dynamical processes that enhance FRB candidate formation likewise contribute to the Type Ia population, which we investigate further in Appendix A.

### 3.2. Delay Time Distributions

A key discriminant among proposed FRB progenitor models is the delay time distribution (DTD), defined as the time between star formation and the FRB. Models in which FRBs are produced promptly after massive star formation, such as magnetars born in core-collapse supernovae (CCSNe), predict short delay times that closely trace the star formation history (SFH) of their host galaxies (e.g., Metzger et al. 2017; Margalit et al. 2019; Bochenek et al. 2020; CHIME/FRB Collaboration et al. 2020). In contrast, models of delayed channels, such as AIC of massive white dwarfs or compact object mergers, predict longer delay times, leading to a rate that lags behind the SFH (e.g., Nomoto & Kondo 1991; Schwab 2021; Wang et al. 2016). The detection of FRBs in a variety of host galaxies (e.g., Gordon et al. 2025; Horowitz & Margalit 2025), including some in quiescent elliptical galaxies (e.g., Shah et al. 2025; Eftekhari et al. 2025) and globular clusters (Bhardwaj et al. 2021b; Kirsten et al. 2022), lends evidence for a delayed FRB formation channel.

Figure 2 compares the DTDs for the different FRB progenitor classes and compares those formed in isolated binaries (shaded histograms) to those formed in hierarchical triples (dashed histograms) across three metallicities:  $Z = Z_{\odot}$ ,  $0.1 Z_{\odot}$ , and  $0.01 Z_{\odot}$ . The three columns correspond to distinct progenitor classes, including double CO WD mergers (*left*), mergers containing one massive ( $> 0.85 M_{\odot}$ ) WD and another CO WD (*middle*), and merger-induced collapse or AIC of an O/Ne WD with any companion (*right*).

The left and middle column of Figure 2 shows that WD+WD mergers from triples exhibit a broader DTD than those from isolated binaries, with a tail extending to  $\gtrsim 8$  Gyr at solar metallicity. At solar metallicity, both the total number of WD+WD mergers and their typical delay times are larger in triples than in isolated binaries. This arises because many inner binaries begin with wide orbits ( $P_{\text{in}} \sim 10^4$  days) that were unlikely to interact in isolation. In hierarchical triples, however, secular Kozai-Lidov oscillations driven by the tertiary excite the inner binary's eccentricity. Once the periastron shrinks sufficiently, tidal friction becomes effective, dissipating orbital energy and gradually circularizing and shrinking the orbit to  $P_{\text{in}} \sim 10$  days. This tidal-assisted hardening channel creates new WD+WD binaries that even-

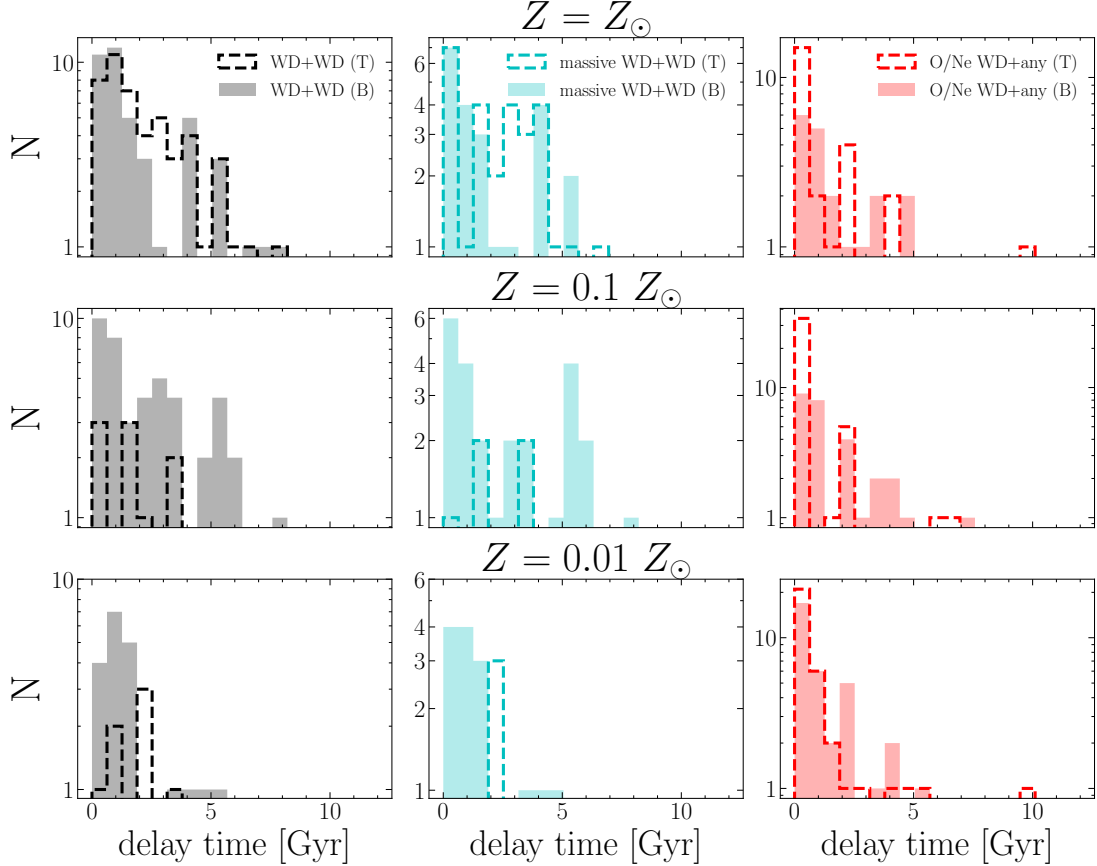


**Figure 2.** Predicted delay time distributions of binary mergers in isolated binaries (filled histograms) and triples (dashed histograms) for various metallicities. We show the results for the different FRB progenitor candidates, including all double WD mergers, double WD mergers including one massive WD, and O/Ne WD+any (including MS or RG) mergers, from left to right. The different rows show different metallicity models.

tually merge, which would not exist in isolated binary evolution. The longer delay times are a natural consequence of this pathway: these systems require multiple stages—first secular eccentricity excitation, then tidal circularization, followed by stellar evolution and mass transfer to the WD+WD stage, then gravitational wave inspiral until merger. On the other hand, some are eccentric WD+WD collisions that occur after a few Gyr, also extending the delay time. In contrast, isolated binaries that merge typically begin much closer, interact earlier through mass transfer, and therefore merge on shorter timescales. Triples thus preferentially populate the long-delay tail of the distribution while also boosting the overall number of WD+WD mergers at solar  $Z$ .

At very low metallicity (e.g.,  $\lesssim 0.1 Z_{\odot}$ ), we find fewer mergers in triples than in isolated binaries across all classes of FRB candidates. This difference arises from both orbital dynamics and stellar evolution. As before, triple inner binaries are often driven to short periods ( $P_{\text{in}} \lesssim 10$  days) by early EKL cycles followed by tidal circularization. At such close separations, subsequent stellar evolution occurs under conditions very

different from solar metallicity. Because reduced line-driven winds at low  $Z$  lead to larger pre-WD masses and more compact stellar radii, mass transfer is typically initiated when the mass ratio is extreme ( $q \ll 1$ ). A smaller mass ratio makes unstable mass transfer more likely, thus leading to a larger fraction of mergers. In contrast, isolated binaries at the same metallicity cover a broader range of initial periods ( $P_{\text{orb}} \in 10 - 10^3$  days). Many remain wide enough to avoid early tidal shrinkage, initiating mass transfer later, at wider orbits and mass ratios closer to unity, making survival more likely. As a result, while triples at solar  $Z$  enhance the WD+WD merger rate, at low  $Z$  their early hardening actually suppresses the production of FRB candidate systems. However, the triple dynamical channels (2 and 3 in Section 3.1) crucially remain pronounced at low  $Z$  because they are minimally dependent on metallicity, thus contributing to late-time FRB candidate formation in low metallicity environments.

The rightmost column of Figure 2 shows the O/Ne WD+any channel, dominated by WD+MS and WD+RG mergers, which can yield an AIC if sufficient

mass is accreted. The DTDs in both triples and binaries are strongly weighted toward short delays ( $< 1$  Gyr) at all metallicities, with a modest tail to longer times due to some O/Ne WD that only accrete when the secondary evolves to become a giant, which requires a few Gyr on average.

To summarize, triples and binaries predict qualitatively different delay time distributions for WD+WD mergers, with triples generally producing more mergers with longer delay times at all metallicities. At high  $Z$ , tertiary-induced eccentricity excitation and tidal hardening create WD+WD systems that would not merge in isolation, boosting both the total number of events and the delayed tail of the DTD. At low  $Z$ , however, reduced stellar winds and more massive progenitors make mass transfer less stable, leading to more mergers during common envelope evolution, thus suppressing WD mergers in triples. The surviving systems are dominated by dynamical eccentric collisions, which are rare but extremely delayed, creating an observable signature of the triple channel. Furthermore, the AIC of O/Ne WDs as FRB candidates shows a relatively delayed DTD as well in both binaries and triples (right panel of Figure 2) because this channel often requires the secondary star to evolve into a giant to fill its Roche Lobe and begin mass transfer onto the O/Ne WD. These metallicity- and dynamics-dependent contrasts underscore the importance of including triple dynamics when modeling FRB progenitors. In the next section, we translate these distributions into volumetric FRB rates by convolving them with the cosmic star formation history, enabling predictions for the redshift evolution of the FRB population.

### 3.3. Redshift Evolution

As the number of observed FRBs grows, especially at cosmological distances, their event rates at various redshifts will become increasingly constrained. Similar constraints were made for SNe Ia supernovae (e.g., Maoz & Graur 2017), leading to sharp constraints on their progenitor channels (e.g., Maoz & Mannucci 2012; Maoz et al. 2012; Liu et al. 2023).

At present, however, the observed FRB sample is dominated by low-redshift sources and by intrinsic uncertainties, such as the DM-redshift relation, luminosity function, and fraction of repeating versus non-repeating sources. These make it challenging to distinguish models that trace the cosmic star formation history from those that assume delayed DTDs (e.g., Tang et al. 2023; Lei et al. 2025; Meng & Deng 2025). Namely, while the local ( $z \approx 0$ ) FRB volumetric rate and luminosity function are jointly constrained to some extent, the overall

redshift evolution of this rate remains poorly understood and model-dependent.

Current and upcoming wide-field radio surveys, notably CHIME/FRB (CHIME/FRB Collaboration et al. 2021), DSA-110 (Law et al. 2024), and the future DSA-2000 (Hallinan et al. 2019), are poised to dramatically improve FRB detection beyond  $z \sim 0.5$ . We translate the number of FRB candidates formed per system (binary or triple) into a rate assuming typical stellar multiplicities. Namely, we take  $f_{\text{binary}} = 34\%$  as the percentage of *all stars* formed that reside in isolated binaries<sup>7</sup>. We also assume that  $f_{\text{triple}} = 11.6\%$  of all stars reside in triples (Moe & Di Stefano 2017; Shariat et al. 2025a), derived using a publicly available tool<sup>8</sup> that samples mock stellar populations with singles, binaries, and triples consistent with observed multiplicity statistics. Note that our sampling intrinsically assumes a Kroupa initial mass function (Kroupa et al. 1993) for all stars. Thus, the Galactic rate from the triple channel can be estimated using:

$$\Gamma \approx 10^{-3} \text{ yr}^{-1} \left( \frac{\text{SFR}}{2 \text{ yr}^{-1}} \right) \left( \frac{f_{\text{triple}}}{0.1} \right) \left( \frac{f_{\text{channel}}}{5 \times 10^{-3}} \right), \quad (3)$$

with a similar equation for binary systems by replacing  $f_{\text{triple}}$  with  $f_{\text{binary}}$ . Here,  $f_{\text{channel}}$  is the fraction of FRB candidates formed per stellar system (binary or triples), taken from Table 1. SFR is the star formation rate, taken to be  $\approx 2$  stars per year, assuming a Kroupa IMF and true SFR of  $\sim 1 \text{ M}_\odot \text{ yr}^{-1}$ . If we assume a number density of  $0.02 \text{ Mpc}^{-3}$  for Milky-Way-like galaxies, we estimate a local volumetric rate of

$$\mathcal{R}_0 \approx 10^4 \text{ Gpc}^{-3} \text{ yr}^{-1} \left( \frac{\Gamma}{10^{-3} \text{ yr}^{-1}} \right). \quad (4)$$

Note that the above is a heuristic estimation using typical values and assuming typical values for SFR and  $f_{\text{channel}}$  from Table 1. Nonetheless, it demonstrates that the typical rates from the triple channel are comparable to the observed local rates. We discuss this further below.

We translate the full delay time distributions from our binary/triple simulations (Figure 2) into FRB source rates as a function of redshift by convolving each DTD with the cosmic star formation rate density (SFRD) from Madau & Dickinson (2014):

$$\psi(z) = 0.015 \frac{(1+z)^{2.7}}{1 + [(1+z)/2.9]^{5.6}} \text{ M}_\odot \text{ yr}^{-1} \text{ Mpc}^{-3}. \quad (5)$$

<sup>7</sup> Note this fraction is among all stars, not systems.

<sup>8</sup> [https://github.com/cheyanneshariat/gaia\\_triples](https://github.com/cheyanneshariat/gaia_triples)

Additionally, we combine all of the metallicity models by weighting by the cosmic mean metallicity evolution from (Madau & Fragos 2017):

$$\log_{10}(\bar{Z}/Z_{\odot}) = 0.153 - 0.074z^{1.34}. \quad (6)$$

Figure 3 shows the resulting FRB source rates and their redshift evolution for the WD+WD (black), massive WD+WD (cyan), and O/Ne WD+any (red) merger scenarios. The top panel displays the individual curves for isolated binaries (dashed) and triples (solid), while the bottom panels present the combined rate, assuming a realistic stellar population with both binaries and triples, using the multiplicity fractions described above.

The binary WD+WD channel broadly tracks the cosmic star formation history (SFH), reflecting their typically short delay times. By contrast, mergers formed in triples are systematically shifted to lower redshift due to longer typical delays ( $\gtrsim 1$  Gyr). For instance, the WD+WD merger rate in triples peaks at  $z \approx 1.0$ , whereas the equivalent binary channel peaks at  $z \approx 1.9$ . This systematic offset is robust across metallicities (e.g., Figure 2), with all double-degenerate triple channels peaking near  $z \sim 1$ . Therefore, if triples contribute significantly to the merger rate, our models predict an observed excess around  $z = 1$  relative to binary-only predictions (top panel of Figure 3).

Overall, the different delay signatures are important for interpreting FRB host galaxy demographics: prompt channels (short delays) closely track the cosmic star formation history, and thus should dominate in galactic hosts with recent star formation at  $z \lesssim 1$ , consistent with some recent host galaxy identifications (e.g., Bhandari et al. 2020; Heintz et al. 2020; Shah et al. 2025; Eftekhari et al. 2025; Gordon et al. 2025).

It is worth emphasizing that the absolute local FRB volumetric event rate remains uncertain, both in the value and its redshift evolution, due to uncertainties in the fluence completeness and DM-redshift relations (e.g., James et al. 2022; Meng & Deng 2025). Nevertheless, combining the DTD analysis with the convolved redshift-dependent rates demonstrates two robust trends: (i) triple evolution broadens the temporal window over which FRBs can occur, shifting a significant fraction to later cosmic times, and (ii) metallicity introduces distinct differences between binary and triple channels. Together, these results provide a natural framework for understanding why FRBs are found in both young, star-forming galaxies and older, passive hosts, and suggest that surveys targeting low-metallicity environments or  $z \sim 1$  systems will be especially valuable for constraining progenitor models. Table 2 summarizes the main characteristics for FRB rate evolution,

including the local rate ( $\mathcal{R}_0$ ), the peak redshift ( $z_{\text{peak}}$ ), and the peak rate ( $\mathcal{R}_{\text{peak}}$ ).

To compare our predictions with observations, we compile several recent estimates of the FRB volumetric rate (colored points in Figure 3). It is important to note that these rates are not direct measurements: inferring an event rate requires assumptions about the FRB luminosity function, source population, and survey selection effects, all of which remain highly uncertain. Additional uncertainties arise from the poorly constrained mapping between DM and redshift, and from the treatment of repeating sources, which are either excluded, down-weighted, or counted as single events depending on the analysis. Thus, the published estimates should be viewed as model-dependent and approximate, rather than definitive measurements of the FRB rate. We briefly describe each below.

Different studies using different samples and methodologies yield local FRB rates that vary by up to an order of magnitude. Chen et al. (2024), by fitting 474 apparently non-repeating CHIME/FRB events, find a monotonically declining formation rate  $\rho(z) \propto (1+z)^{-4.9 \pm 0.3}$  with a local rate of  $1.1 \times 10^4 \text{ Gpc}^{-3} \text{ yr}^{-1}$ . Meng & Deng (2025), by incorporating instrumental selection effects with Monte Carlo simulations of CHIME data, report higher rates of  $2.3_{-1.2}^{+2.4} \times 10^5$  and  $3.9_{-1.2}^{+2.5} \times 10^4 \text{ Gpc}^{-3} \text{ yr}^{-1}$  for pivot energies above  $10^{38}$  and  $10^{39}$  erg, respectively; we adopt the latter for consistency with other works. James et al. (2022) use ASKAP and Parkes to estimate  $8.7_{-3.9}^{+1.7} \times 10^4 \text{ Gpc}^{-3} \text{ yr}^{-1}$  above  $10^{39}$  erg. Shin et al. (2023) fit fluence and DM distributions from CHIME, finding  $7.3_{-3.8}^{+8.8} \times 10^4 \text{ Gpc}^{-3} \text{ yr}^{-1}$ . Finally, Hashimoto et al. (2022), analyzing 164 non-repeating CHIME events, derive a lower local rate of  $1.5 \times 10^4 \text{ Gpc}^{-3} \text{ yr}^{-1}$  at  $0.05 < z \leq 0.3$ .

The above estimations are included in Figure 3. In general, the predicted rates for each scenario reside around  $\approx 1 \times 10^4 \text{ Gpc}^{-3} \text{ yr}^{-1}$  at  $z = 0$  and  $\approx 5 \times 10^4 \text{ Gpc}^{-3} \text{ yr}^{-1}$  at  $z \approx 1-2$ , when summing the contribution from both binaries and triples. These estimates are broadly consistent with observations, particularly Shin et al. (2023) and Hashimoto et al. (2022). However, since we report formation rates of candidate FRB progenitors from our simulations, rather than actual *event* rates, the unknown fraction of repeating sources complicates the comparison and makes our reported rates strictly lower limits.

#### 4. CONCLUSIONS

In this work, we explore the formation of FRB progenitors through white dwarf mergers/collapse in binary and triple star systems. Using detailed three-body

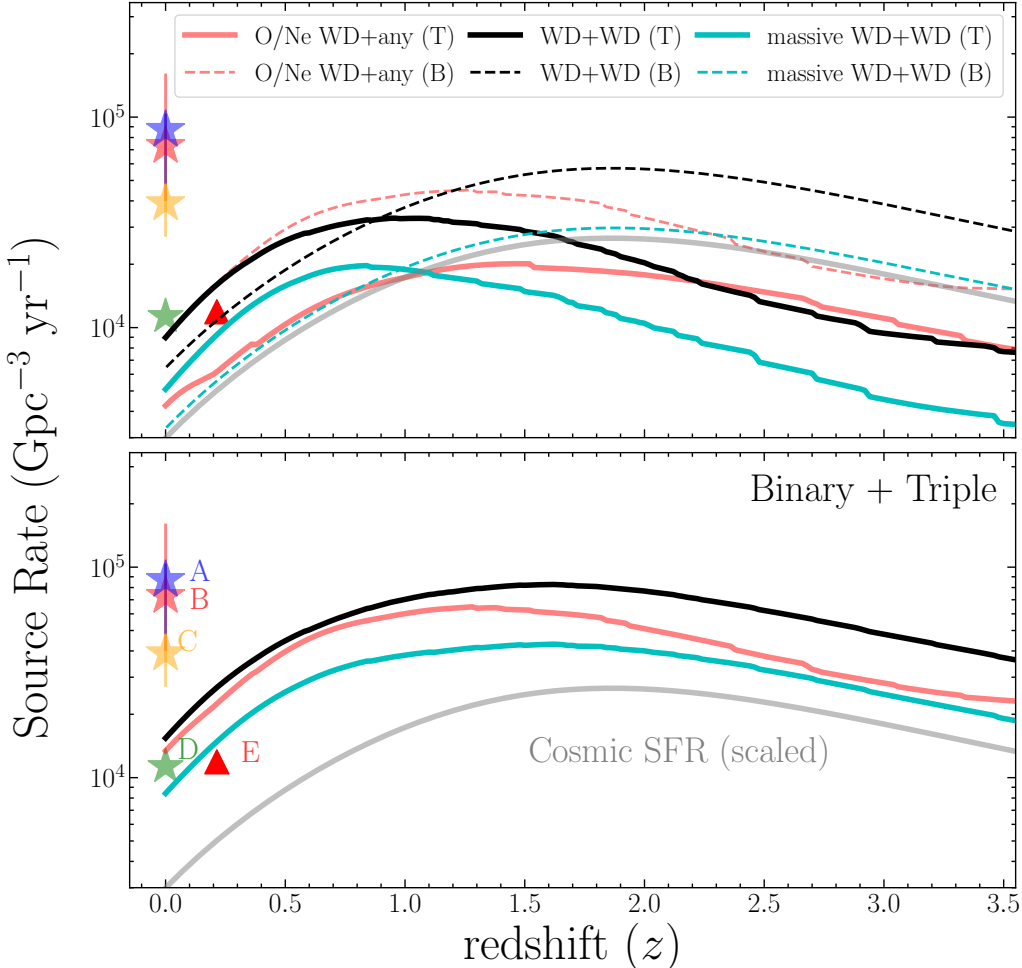


**Figure 3.** Predicted redshift evolution of FRB source rates in both triples and isolated binaries. The top row shows the distinct contribution from triples (solid lines) and binaries (dashed lines) for different collapse scenarios, while the bottom row combines both channels. In each panel, we show three different FRB progenitor scenarios, including O/Ne WD + any secondary (red), CO WD+WD (black), and massive WD+WD (blue). The bottom panel also contains the cosmic star formation history in gray and various estimates of the local FRB event rate at  $z \approx 0$ , derived by modeling observations. These include James et al. (2022) (A), Shin et al. (2023) (B), Meng & Deng (2025) (C), Chen et al. (2024) (D), and Hashimoto et al. (2022) (E). Note that the rates from our models include only unique FRB candidates, without accounting for repeaters.

simulations combined with binary population synthesis, we trace the evolutionary pathways leading to classes of mergers and accretion-induced collapse events, and investigate their implications for the FRB population. Our main results are summarized as follows:

1. *Formation pathways of FRBs in triples:* Hierarchical triples open new formation pathways to FRB candidates that are inaccessible in isolated binaries (Figure 1). In particular, eccentricity excitation through the EKL mechanism can shrink wide inner binaries that would otherwise remain detached, producing elevated rates of binary mass transfer and thus the collapse of super-Chandrasekhar WDs to potential FRB-emitting young neutron stars. At solar metallicity, this channel substan-

tially boosts the total number of mergers relative to isolated binary evolution, while at low metallicity ( $Z \lesssim 0.1 Z_{\odot}$ ), the enhancement is suppressed due to increased unstable mass transfer rates from larger pre-WD masses. However, the dynamically-induced merger channel, where a tertiary triggers a WD+WD or WD+MS collision in the inner binary, is independent of metallicity and provides an important contribution with larger typical delay times ( $\gtrsim 1$  Gyr).

2. *Delay times:* The DTDs of the FRB candidates in triples are systematically broader than those from isolated binaries (Figure 2). At solar metallicity, tertiary-driven tidal shrinkage produces WD+WD mergers on long timescales, extending the DTD

tail to  $\gtrsim 8$  Gyr. At low metallicity, while the total number of triple mergers decreases, the surviving systems are dominated by eccentric WD+WD collisions, which are independent of metallicity and occur on very long timescales. Indeed, FRB hosts show a weak-to-null metallicity preference (e.g., Yamasaki et al. 2025).

3. *Host Environments:* Because most FRB candidates formed through secular three-body dynamics have longer average delay times, they are not expected to trace ongoing star formation in all cases. Instead, a substantial fraction will reside among older stellar populations, including quiescent host galaxies or galactic halos. Thus, triple formation can naturally account for the observations of FRBs in a variety of host environments (e.g., Eftekhari et al. 2025; Shah et al. 2025; Gordon et al. 2025).
4. *Rates and Redshift evolution:* By convolving the DTDs with the cosmic star formation history, we predict the redshift evolution of the FRB rate (Figure 3). Binary-driven WD+WD merger channels largely track the star formation rate. This systematic offset is a robust prediction of the triple scenario: if WD+WD mergers in triples contribute significantly to FRBs relative to other channels, their observed rate distribution should favor lower redshifts. For the AIC scenario, we find that both binary and triple scenarios lead to moderately delayed distribution. Combining both binary and triple channels across metallicities, our models predict a local FRB candidate source rate  $R_0 \approx 2 \times 10^4 \text{ Gpc}^{-3} \text{ yr}^{-1}$  (Figure 3), comparable to recent observations (see also Table 2).
5. *Implications for SNe Ia:* Using the same simulations, we revisited the role of WD mergers in producing SNe Ia through both binaries and triples. By only considering double-degenerate mergers with a massive CO WD primary (including He WD secondaries), as motivated by detonation models and observations, we find that triples extend the delay-time distribution and yield SNe Ia at roughly twice the efficiency of isolated binaries ( $12 \times 10^{-4}$  vs.  $6 \times 10^{-4}$  SNe  $M_{\odot}^{-1}$ ; Figure 4). Combining both binary and triple channels, we predict an overall efficiency of  $\approx 2 \times 10^{-3}$  SNe  $M_{\odot}^{-1}$ , a

local volumetric rate of  $\approx 3 \times 10^4 \text{ Gpc}^{-3} \text{ yr}^{-1}$ , and a redshift evolution all in good agreement with observations (Appendix A). These results indicate that triples are an essential component of the SNe Ia progenitor population, although future work is needed to assess the theoretical uncertainties in modeling Type Ia progenitors.

Our results highlight the distinct role of triple dynamics in forming candidate FRB progenitors. Testing these predictions observationally offers a promising path to identifying the dominant FRB formation channels. Arcsecond-scale localizations are already constraining host-galaxy properties, while sub-arcsecond positions will continue to pinpoint the local environment of FRBs, together providing powerful clues to their origins. The discovery of a nearby stellar companion to an FRB source would further support accretion-induced collapse pathways. Upcoming wide-field surveys such as CHIME/FRB Catalog 2, CHORD, DSA-110, and DSA-2000 will expand FRB samples, enabling precise measurements of rates, luminosity functions, repeater fractions, and redshift evolution. These advances will provide the statistical power needed to test predictions and to distinguish the relative contributions of binaries, triples, and other FRB progenitor pathways.

## 5. ACKNOWLEDGMENTS

We thank the 56th Annual Meeting of the Division on Dynamical Astronomy (DDA) for sparking early conversations about the topic. We also thank Chang Liu, Kaitlyn Shin, Kenzie Nimmo, and Barack Zackay for valuable discussions.

C.S. acknowledges support from the Joshua and Beth Friedman Foundation Fund and the Department of Energy Computational Science Graduate Fellowship. This material is based upon work supported by the U.S. Department of Energy, Office of Science, Office of Advanced Scientific Computing Research, under Award Number DE-SC0026073. C.S.Y. acknowledges support from the Natural Sciences and Engineering Research Council of Canada (NSERC) DIS-2022-568580 and the Alfred P. Sloan Foundation. S.N. acknowledges the partial support of NSF-BSF grant AST-2206428 and NASA XRP grant 80NSSC23K0262, as well as Howard and Astrid Preston for their generous support. S.C.R. thanks the CIERA Lindheimer Fellowship for support.

## APPENDIX

### A. TYPE IA SUPERNOVAE

Throughout this study, we have considered mergers of two white dwarfs. A natural extension of our results is to the double-degenerate scenario for Type Ia supernovae (SNe Ia). The role of triples in producing SNe Ia has been explored in several works (e.g., Thompson 2011b; Katz & Dong 2012; Hamers et al. 2013; Hamers & Thompson 2019; Toonen et al. 2018; Michael 2021; Rajamuthukumar et al. 2023), and our simulations with realistic initial conditions allow us to revisit this question. Specifically, we focus on the delay times, rates, and redshift evolution of SNe Ia in both binary and triple channels.

We adopt two criteria for SNe Ia progenitors: (i) mergers between a massive CO WD ( $> 0.85 M_{\odot}$ ) and another WD, including He WDs (which were excluded from our FRB analysis), and (ii) mergers between two CO WDs of any mass. The first channel is deemed the ‘Physical’ channel as it is motivated by explosion models that find stable detonations in C/O+He WD systems with massive primaries (e.g., Guillochon et al. 2010; Ruiter et al. 2011; Shen et al. 2018, 2021), while the second follows the canonical double-degenerate model.

A recent triple study by Rajamuthukumar et al. (2023) found that the SN Ia rate from triples is comparable to that from binaries, both  $\sim 3 \times 10^{-4}$  SNe  $M_{\odot}^{-1}$ , which combined is still a factor of a few less than an observed estimate of the local rate  $\sim 13 \times 10^{-4}$  SNe  $M_{\odot}^{-1}$ . However, they allow *all* CO+He WD mergers to produce SNe Ia, irrespective of mass. In fact, 96 – 99% of the SNe Ia in their binary/triple evolution models arise from such mergers, making it imperative to their results. This likely overestimates the contribution, since hydrodynamical simulations suggest that only sufficiently massive ( $\gtrsim 0.85 M_{\odot}$ ) primaries can reproduce the observed luminosities of most SNe Ia (e.g., Pakmor et al. 2012; Shen et al. 2018; Hoeflich et al. 2017), unlike the typical WD mass of  $\sim 0.6 M_{\odot}$  while likely dominates the Type Ia progenitors in their simulations. Furthermore, their simulations were truncated at a maximum wall time of 5 hr, which can make it difficult to capture the long-term dynamics that often drive late-time triple-induced mergers.

Guided by these results, we adopt two models. An ‘Inclusive’ model that considers all CO+CO WD mergers as potential SNe Ia progenitors, independent of component masses. The second is a ‘Physical’ model which requires that the primary be a massive CO WD ( $> 0.85 M_{\odot}$ ), consistent with explosion models that reproduce the typical luminosities of normal SNe Ia (e.g., Shen 2025, and references therein).

In Figure 4, we show the predicted redshift evolution of the SN Ia rate from binaries and triples. The top panel highlights that in the Inclusive model, binaries typically produce shorter delay times, while triple-induced mergers extend the distribution to longer delays. Namely, despite there being fewer triples than binaries by a factor of 3, triples still contribute more significantly to CO+CO white dwarf mergers at  $z \lesssim 1$  than isolated binaries.

In the Physical model, where only massive CO WDs are included, the shape of the rate evolution is similar in both binaries and triples. The bottom panel, combining binaries and triples in a 3:1 ratio, shows that both models are consistent with observed SN Ia rates across redshift (compiled by Maoz & Graur 2017). This predicts a local volumetric Ia rate of  $\mathcal{R}_{0,\text{Ia}} \approx 3 \times 10^{-4}$  Gpc $^{-3}$  yr $^{-1}$ . Importantly, both the estimated rate and redshift dependence of our predicted rates align with current observational constraints.

In terms of efficiency of Ia formation, we find that the binary channel contributes  $6 \times 10^{-4}$  SNe  $M_{\odot}^{-1}$  and triples contribute  $1.5 \times 10^{-3}$  SNe  $M_{\odot}^{-1}$ . In total, this leads to an estimate of  $\sim 2 \times 10^{-3}$  SNe  $M_{\odot}^{-1}$ , consistent with the observed rate of  $(1.3 \pm 0.2) \times 10^{-3}$  SNe  $M_{\odot}^{-1}$  (Maoz et al. 2012).

Note that modeling SNe Ia progenitors through binary evolution carries substantial theoretical uncertainties, spanning common-envelope physics, mass transfer stability, and explosion mechanisms (e.g., Claeys et al. 2014; Liu et al. 2023). Our results are therefore uncertain. Instead, we demonstrate that, under reasonable assumptions and physically motivated definitions of SNe Ia progenitors, including both binary and triple formation pathways, yields rates and redshift evolution of SNe Ia are broadly consistent with the literature. A more detailed exploration of the binary physics and explosion criteria will be necessary in future work.

### B. REDSHIFT EVOLUTION OF FRB CANDIDATES

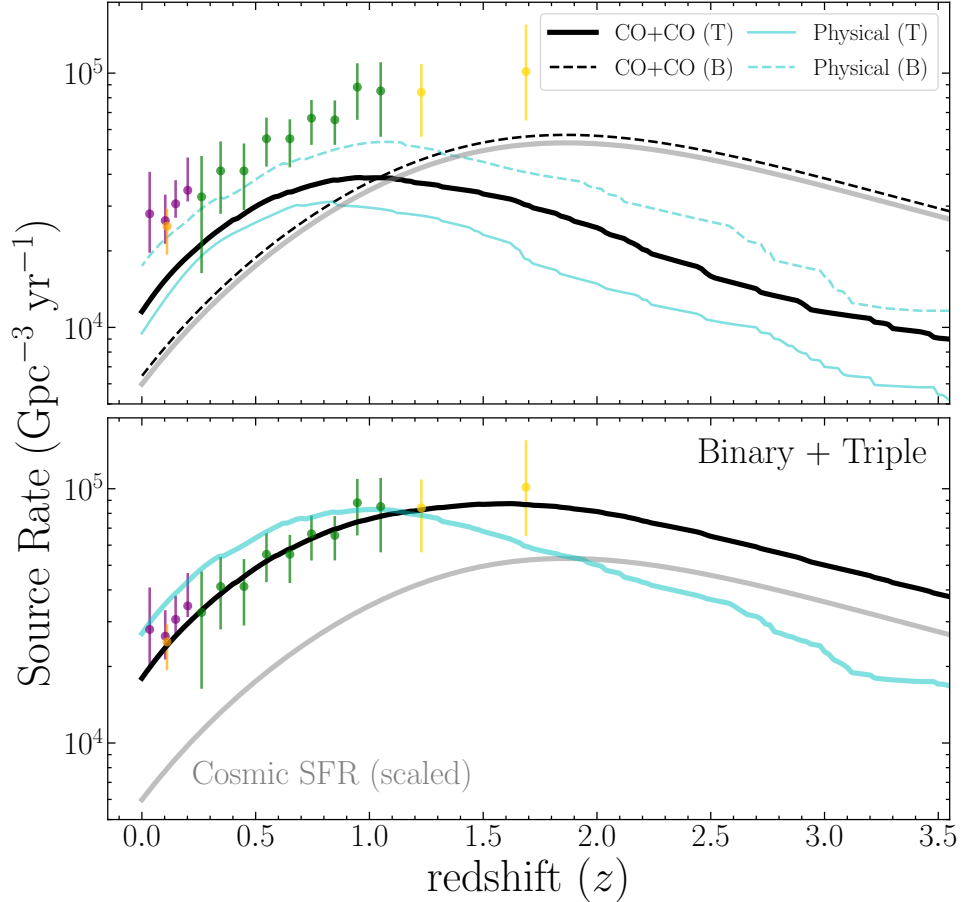


**Figure 4.** Predicted rates and redshift evolution of Type Ia supernova from a stellar population containing both binaries and triples. The top panel shows the individual rates of triples (solid lines) and isolated binaries (dashed lines), while the bottom panel shows their combined rates. We assume two different Type Ia progenitor models: one including all CO + CO WD mergers (black), and one that only includes massive CO WD mergers ( $> 0.9 M_{\odot}$ ) with either a CO WD or a He WD (blue). The bottom panels also displays observed rates from Dilday et al. (2010) (purple), Graur & Maoz (2013) (orange), Perrett et al. (2012) (green), and Graur et al. (2011) (yellow).

**Table 2.** Peak redshift and FRB rates for all channels, modes, and metallicities. Rates are in  $\text{Gpc}^{-3} \text{ yr}^{-1}$ ; ‘Total’ sums triple and binary curves before measuring peaks.

Channel	Metallicity	Triple			Binary			Total		
		$\mathcal{R}_0$ [ $\text{Gpc}^{-3} \text{ yr}^{-1}$ ]	$\mathcal{R}_{\text{peak}}$	$z_{\text{peak}}$	$\mathcal{R}_0$ [ $\text{Gpc}^{-3} \text{ yr}^{-1}$ ]	$\mathcal{R}_{\text{peak}}$	$z_{\text{peak}}$	$\mathcal{R}_0$ [ $\text{Gpc}^{-3} \text{ yr}^{-1}$ ]	$\mathcal{R}_{\text{peak}}$	$z_{\text{peak}}$
<b>WD+WD</b>	combined $Z$	$1.2 \times 10^4$	$3.9 \times 10^4$	0.96	$6.4 \times 10^3$	$5.7 \times 10^4$	1.86	$1.8 \times 10^4$	$8.7 \times 10^4$	1.62
	$Z = Z_{\odot}$	$1.2 \times 10^4$	$4.1 \times 10^4$	1.04	$6.4 \times 10^3$	$5.7 \times 10^4$	1.86	$1.9 \times 10^4$	$9.0 \times 10^4$	1.62
	$Z = 0.1 Z_{\odot}$	$4.0 \times 10^3$	$1.3 \times 10^4$	1.02	$6.4 \times 10^3$	$5.7 \times 10^4$	1.86	$1.0 \times 10^4$	$6.7 \times 10^4$	1.78
	$Z = 0.01 Z_{\odot}$	$3.7 \times 10^3$	$1.2 \times 10^4$	1.02	$3.0 \times 10^3$	$2.7 \times 10^4$	1.86	$6.7 \times 10^3$	$3.5 \times 10^4$	1.70
<b>O/Ne WD+any</b>	combined $Z$	$4.2 \times 10^3$	$2.0 \times 10^4$	1.52	$9.0 \times 10^3$	$4.5 \times 10^4$	1.30	$1.3 \times 10^4$	$6.5 \times 10^4$	1.30
	$Z = Z_{\odot}$	$4.3 \times 10^3$	$2.0 \times 10^4$	1.46	$9.2 \times 10^3$	$4.5 \times 10^4$	1.28	$1.3 \times 10^4$	$6.5 \times 10^4$	1.28
	$Z = 0.1 Z_{\odot}$	$4.3 \times 10^3$	$2.0 \times 10^4$	1.46	$9.2 \times 10^3$	$4.5 \times 10^4$	1.28	$1.3 \times 10^4$	$6.5 \times 10^4$	1.28
	$Z = 0.01 Z_{\odot}$	$4.3 \times 10^3$	$2.0 \times 10^4$	1.46	$9.2 \times 10^3$	$4.5 \times 10^4$	1.28	$1.3 \times 10^4$	$6.5 \times 10^4$	1.28
<b>massive WD+WD</b>	combined $Z$	$5.5 \times 10^3$	$2.2 \times 10^4$	0.86	$3.3 \times 10^3$	$3.0 \times 10^4$	1.92	$8.9 \times 10^3$	$4.6 \times 10^4$	1.70
	$Z = Z_{\odot}$	$5.9 \times 10^3$	$2.4 \times 10^4$	0.84	$3.3 \times 10^3$	$2.9 \times 10^4$	1.86	$9.2 \times 10^3$	$4.6 \times 10^4$	1.62
	$Z = 0.1 Z_{\odot}$	$2.1 \times 10^3$	$1.1 \times 10^4$	1.00	$3.7 \times 10^3$	$3.3 \times 10^4$	1.86	$5.9 \times 10^3$	$4.1 \times 10^4$	1.72
	$Z = 0.01 Z_{\odot}$	$1.1 \times 10^3$	$6.9 \times 10^3$	1.32	$2.4 \times 10^3$	$2.1 \times 10^4$	1.86	$3.5 \times 10^3$	$2.8 \times 10^4$	1.74

## REFERENCES

Angelo, I., Naoz, S., Petigura, E., et al. 2022, AJ, 163, 227, doi: [10.3847/1538-3881/ac6094](https://doi.org/10.3847/1538-3881/ac6094)

Antonini, F., Murray, N., & Mikkola, S. 2014, ApJ, 781, 45, doi: [10.1088/0004-637X/781/1/45](https://doi.org/10.1088/0004-637X/781/1/45)

Bannister, K. W., Deller, A. T., Phillips, C., et al. 2019, Science, 365, 565, doi: [10.1126/science.aaw5903](https://doi.org/10.1126/science.aaw5903)

Bassa, C. G., Tendulkar, S. P., Adams, E. A. K., et al. 2017, ApJL, 843, L8, doi: [10.3847/2041-8213/aa7a0c](https://doi.org/10.3847/2041-8213/aa7a0c)

Belczynski, K., Kalogera, V., Rasio, F. A., et al. 2008, ApJS, 174, 223, doi: [10.1086/521026](https://doi.org/10.1086/521026)

Bhandari, S., Keane, E. F., Barr, E. D., et al. 2018, MNRAS, 475, 1427, doi: [10.1093/mnras/stx3074](https://doi.org/10.1093/mnras/stx3074)

Bhandari, S., Sadler, E. M., Prochaska, J. X., et al. 2020, ApJL, 895, L37, doi: [10.3847/2041-8213/ab672e](https://doi.org/10.3847/2041-8213/ab672e)

Bhandari, S., Heintz, K. E., Aggarwal, K., et al. 2022, AJ, 163, 69, doi: [10.3847/1538-3881/ac3aee](https://doi.org/10.3847/1538-3881/ac3aee)

Bhardwaj, M., Kirichenko, A. Y., Michilli, D., et al. 2021a, ApJL, 919, L24, doi: [10.3847/2041-8213/ac223b](https://doi.org/10.3847/2041-8213/ac223b)

Bhardwaj, M., Gaensler, B. M., Kaspi, V. M., et al. 2021b, ApJL, 910, L18, doi: [10.3847/2041-8213/abeaa6](https://doi.org/10.3847/2041-8213/abeaa6)

Bochenek, C. D., Ravi, V., Belov, K. V., et al. 2020, Nature, 587, 59, doi: [10.1038/s41586-020-2872-x](https://doi.org/10.1038/s41586-020-2872-x)

Breivik, K., Mingarelli, C. M. F., & Larson, S. L. 2020, ApJ, 901, 4, doi: [10.3847/1538-4357/abab99](https://doi.org/10.3847/1538-4357/abab99)

Bruni, G., Piro, L., Yang, Y.-P., et al. 2024, Nature, 632, 1014, doi: [10.1038/s41586-024-07782-6](https://doi.org/10.1038/s41586-024-07782-6)

Bruni, G., Piro, L., Yang, Y. P., et al. 2025, A&A, 695, L12, doi: [10.1051/0004-6361/202453233](https://doi.org/10.1051/0004-6361/202453233)

Caiazzo, I., Burdge, K. B., Fuller, J., et al. 2021, Nature, 595, 39, doi: [10.1038/s41586-021-03615-y](https://doi.org/10.1038/s41586-021-03615-y)

Cao, X.-F., Yu, Y.-W., & Zhou, X. 2018, ApJ, 858, 89, doi: [10.3847/1538-4357/aabadd](https://doi.org/10.3847/1538-4357/aabadd)

Chatterjee, S., Law, C. J., Wharton, R. S., et al. 2017, Nature, 541, 58, doi: [10.1038/nature20797](https://doi.org/10.1038/nature20797)

Chen, J. H., Jia, X. D., Dong, X. F., & Wang, F. Y. 2024, ApJL, 973, L54, doi: [10.3847/2041-8213/ad7b39](https://doi.org/10.3847/2041-8213/ad7b39)

CHIME/FRB Collaboration, Andersen, B. C., Bandura, K. M., et al. 2020, Nature, 587, 54, doi: [10.1038/s41586-020-2863-y](https://doi.org/10.1038/s41586-020-2863-y)

CHIME/FRB Collaboration, Amiri, M., Andersen, B. C., et al. 2021, ApJS, 257, 59, doi: [10.3847/1538-4365/ac33ab](https://doi.org/10.3847/1538-4365/ac33ab)

Claeys, J. S. W., Pols, O. R., Izzard, R. G., Vink, J., & Verbunt, F. W. M. 2014, A&A, 563, A83, doi: [10.1051/0004-6361/201322714](https://doi.org/10.1051/0004-6361/201322714)

Combi, L., Siegel, D. M., & Metzger, B. D. 2025, arXiv e-prints, arXiv:2509.19799. <https://arxiv.org/abs/2509.19799>

Conway, L., & Will, C. M. 2024, PhRvD, 110, 083022, doi: [10.1103/PhysRevD.110.083022](https://doi.org/10.1103/PhysRevD.110.083022)

Decoene, V., Kotera, K., & Silk, J. 2021, A&A, 645, A122, doi: [10.1051/0004-6361/202038975](https://doi.org/10.1051/0004-6361/202038975)

Deng, C.-M., Zhong, S.-Q., & Dai, Z.-G. 2021, ApJ, 922, 98, doi: [10.3847/1538-4357/ac30db](https://doi.org/10.3847/1538-4357/ac30db)

Dessart, L., Burrows, A., Livne, E., & Ott, C. D. 2007, ApJ, 669, 585, doi: [10.1086/521701](https://doi.org/10.1086/521701)

Dilday, B., Smith, M., Bassett, B., et al. 2010, ApJ, 713, 1026, doi: [10.1088/0004-637X/713/2/1026](https://doi.org/10.1088/0004-637X/713/2/1026)

Eftekhari, T., Dong, Y., Fong, W., et al. 2025, ApJL, 979, L22, doi: [10.3847/2041-8213/ad9de2](https://doi.org/10.3847/2041-8213/ad9de2)

Eggleton, P. P., Kiseleva, L. G., & Hut, P. 1998, ApJ, 499, 853, doi: [10.1086/305670](https://doi.org/10.1086/305670)

Fong, W.-f., Dong, Y., Leja, J., et al. 2021, ApJL, 919, L23, doi: [10.3847/2041-8213/ac242b](https://doi.org/10.3847/2041-8213/ac242b)

Ford, E. B., Kozinsky, B., & Rasio, F. A. 2000, ApJ, 535, 385, doi: [10.1086/308815](https://doi.org/10.1086/308815)

Fragione, G., & Loeb, A. 2019a, MNRAS, 486, 4443, doi: [10.1093/mnras/stz1131](https://doi.org/10.1093/mnras/stz1131)

—. 2019b, MNRAS, 490, 4991, doi: [10.1093/mnras/stz2902](https://doi.org/10.1093/mnras/stz2902)

Fuller, J., & Lai, D. 2012, MNRAS, 421, 426, doi: [10.1111/j.1365-2966.2011.20320.x](https://doi.org/10.1111/j.1365-2966.2011.20320.x)

García-Berro, E., Lorén-Aguilar, P., Aznar-Siguán, G., et al. 2012, ApJ, 749, 25, doi: [10.1088/0004-637X/749/1/25](https://doi.org/10.1088/0004-637X/749/1/25)

Gordon, A. C., Fong, W.-f., Deller, A. T., et al. 2025, arXiv e-prints, arXiv:2506.06453, doi: [10.48550/arXiv.2506.06453](https://doi.org/10.48550/arXiv.2506.06453)

Graur, O., & Maoz, D. 2013, MNRAS, 430, 1746, doi: [10.1093/mnras/sts718](https://doi.org/10.1093/mnras/sts718)

Graur, O., Poznanski, D., Maoz, D., et al. 2011, MNRAS, 417, 916, doi: [10.1111/j.1365-2966.2011.19287.x](https://doi.org/10.1111/j.1365-2966.2011.19287.x)

Guillochon, J., Dan, M., Ramirez-Ruiz, E., & Rosswog, S. 2010, ApJL, 709, L64, doi: [10.1088/2041-8205/709/1/L64](https://doi.org/10.1088/2041-8205/709/1/L64)

Hallinan, G., Ravi, V., Weinreb, S., et al. 2019, in Bulletin of the American Astronomical Society, Vol. 51, 255, doi: [10.48550/arXiv.1907.07648](https://doi.org/10.48550/arXiv.1907.07648)

Hamers, A. S., Pols, O. R., Claeys, J. S. W., & Nelemans, G. 2013, MNRAS, 430, 2262, doi: [10.1093/mnras/stt046](https://doi.org/10.1093/mnras/stt046)

Hamers, A. S., & Thompson, T. A. 2019, ApJ, 882, 24, doi: [10.3847/1538-4357/ab321f](https://doi.org/10.3847/1538-4357/ab321f)

Hashimoto, T., Goto, T., Chen, B. H., et al. 2022, MNRAS, 511, 1961, doi: [10.1093/mnras/stac065](https://doi.org/10.1093/mnras/stac065)

Heintz, K. E., Prochaska, J. X., Simha, S., et al. 2020, ApJ, 903, 152, doi: [10.3847/1538-4357/abb6fb](https://doi.org/10.3847/1538-4357/abb6fb)

Hoeflich, P., Hsiao, E. Y., Ashall, C., et al. 2017, ApJ, 846, 58, doi: [10.3847/1538-4357/aa84b2](https://doi.org/10.3847/1538-4357/aa84b2)

Holzknecht, L., Naoz, S., & Shariat, C. 2025, arXiv e-prints, arXiv:2509.21452, doi: [10.48550/arXiv.2509.21452](https://doi.org/10.48550/arXiv.2509.21452)

Horowicz, A., & Margalit, B. 2025, arXiv e-prints, arXiv:2504.08038, doi: [10.48550/arXiv.2504.08038](https://doi.org/10.48550/arXiv.2504.08038)

Hurley, J. R., Pols, O. R., & Tout, C. A. 2000, MNRAS, 315, 543, doi: [10.1046/j.1365-8711.2000.03426.x](https://doi.org/10.1046/j.1365-8711.2000.03426.x)

Hurley, J. R., Tout, C. A., & Pols, O. R. 2002, Monthly Notices of the Royal Astronomical Society, 329, 897, doi: [10.1046/j.1365-8711.2002.05038.x](https://doi.org/10.1046/j.1365-8711.2002.05038.x)

Hut, P. 1980, A&A, 92, 167

James, C. W., Prochaska, J. X., Macquart, J. P., et al. 2022, MNRAS, 510, L18, doi: [10.1093/mnrasl/slab117](https://doi.org/10.1093/mnrasl/slab117)

Jewett, G., Kilic, M., Bergeron, P., et al. 2024, ApJ, 974, 12, doi: [10.3847/1538-4357/ad6905](https://doi.org/10.3847/1538-4357/ad6905)

Kashiyama, K., Ioka, K., & Mészáros, P. 2013, ApJL, 776, L39, doi: [10.1088/2041-8205/776/2/L39](https://doi.org/10.1088/2041-8205/776/2/L39)

Katz, B., & Dong, S. 2012, arXiv e-prints, arXiv:1211.4584, doi: [10.48550/arXiv.1211.4584](https://doi.org/10.48550/arXiv.1211.4584)

Kawka, A., Vennes, S., Schmidt, G. D., Wickramasinghe, D. T., & Koch, R. 2007, ApJ, 654, 499, doi: [10.1086/509072](https://doi.org/10.1086/509072)

Kepler, S. O., Pelisoli, I., Jordan, S., et al. 2013, MNRAS, 429, 2934, doi: [10.1093/mnras/sts522](https://doi.org/10.1093/mnras/sts522)

Kirsten, F., Marcote, B., Nimmo, K., et al. 2022, Nature, 602, 585, doi: [10.1038/s41586-021-04354-w](https://doi.org/10.1038/s41586-021-04354-w)

Knigge, C., Toonen, S., & Boekholt, T. C. N. 2022, MNRAS, 514, 1895, doi: [10.1093/mnras/stac1336](https://doi.org/10.1093/mnras/stac1336)

Kozai, Y. 1962, AJ, 67, 591, doi: [10.1086/108790](https://doi.org/10.1086/108790)

Kremer, K., Fuller, J., Piro, A. L., & Ransom, S. M. 2023, MNRAS, 525, L22, doi: [10.1093/mnrasl/slad088](https://doi.org/10.1093/mnrasl/slad088)

Kremer, K., Piro, A. L., & Li, D. 2021, ApJL, 917, L11, doi: [10.3847/2041-8213/ac13a0](https://doi.org/10.3847/2041-8213/ac13a0)

Kroupa, P., Tout, C. A., & Gilmore, G. 1993, MNRAS, 262, 545, doi: [10.1093/mnras/262.3.545](https://doi.org/10.1093/mnras/262.3.545)

Law, C. J., Sharma, K., Ravi, V., et al. 2024, ApJ, 967, 29, doi: [10.3847/1538-4357/ad3736](https://doi.org/10.3847/1538-4357/ad3736)

Lei, Q.-Z., Wang, X.-Z., & Deng, C.-M. 2025, arXiv e-prints, arXiv:2507.23122, doi: [10.48550/arXiv.2507.23122](https://doi.org/10.48550/arXiv.2507.23122)

Lidov, M. L. 1962, Planet. Space Sci., 9, 719, doi: [10.1016/0032-0633\(62\)90129-0](https://doi.org/10.1016/0032-0633(62)90129-0)

Liebert, J., Bergeron, P., & Holberg, J. B. 2003, AJ, 125, 348, doi: [10.1086/345573](https://doi.org/10.1086/345573)

Liu, Z.-W., Roepke, F. K., & Han, Z. 2023, arXiv e-prints, arXiv:2305.13305, doi: [10.48550/arXiv.2305.13305](https://doi.org/10.48550/arXiv.2305.13305)

Lorimer, D. R., Bailes, M., McLaughlin, M. A., Narkevic, D. J., & Crawford, F. 2007, Science, 318, 777, doi: [10.1126/science.1147532](https://doi.org/10.1126/science.1147532)

Lu, W., Beniamini, P., & Kumar, P. 2022, MNRAS, 510, 1867, doi: [10.1093/mnras/stab3500](https://doi.org/10.1093/mnras/stab3500)

Madau, P., & Dickinson, M. 2014, ARA&A, 52, 415, doi: [10.1146/annurev-astro-081811-125615](https://doi.org/10.1146/annurev-astro-081811-125615)

Madau, P., & Fragos, T. 2017, ApJ, 840, 39, doi: [10.3847/1538-4357/aa6aff9](https://doi.org/10.3847/1538-4357/aa6aff9)

Maoz, D., & Graur, O. 2017, ApJ, 848, 25, doi: [10.3847/1538-4357/aa8b6e](https://doi.org/10.3847/1538-4357/aa8b6e)

Maoz, D., & Mannucci, F. 2012, PASA, 29, 447, doi: [10.1071/AS11052](https://doi.org/10.1071/AS11052)

Maoz, D., Mannucci, F., & Brandt, T. D. 2012, MNRAS, 426, 3282, doi: [10.1111/j.1365-2966.2012.21871.x](https://doi.org/10.1111/j.1365-2966.2012.21871.x)

Marcote, B., Paragi, Z., Hessels, J. W. T., et al. 2017, ApJL, 834, L8, doi: [10.3847/2041-8213/834/2/L8](https://doi.org/10.3847/2041-8213/834/2/L8)

Marcote, B., Nimmo, K., Hessels, J. W. T., et al. 2020, Nature, 577, 190, doi: [10.1038/s41586-019-1866-z](https://doi.org/10.1038/s41586-019-1866-z)

Mardling, R. A., & Aarseth, S. J. 2001, MNRAS, 321, 398, doi: [10.1046/j.1365-8711.2001.03974.x](https://doi.org/10.1046/j.1365-8711.2001.03974.x)

Margalit, B., Berger, E., & Metzger, B. D. 2019, ApJ, 886, 110, doi: [10.3847/1538-4357/ab4c31](https://doi.org/10.3847/1538-4357/ab4c31)

Margalit, B., & Metzger, B. D. 2018, ApJL, 868, L4, doi: [10.3847/2041-8213/aaedad](https://doi.org/10.3847/2041-8213/aaedad)

Meng, M., & Deng, C.-M. 2025, A&A, 698, A127, doi: [10.1051/0004-6361/202451250](https://doi.org/10.1051/0004-6361/202451250)

Metzger, B. D., Berger, E., & Margalit, B. 2017, ApJ, 841, 14, doi: [10.3847/1538-4357/aa633d](https://doi.org/10.3847/1538-4357/aa633d)

Michaely, E. 2021, MNRAS, 500, 5543, doi: [10.1093/mnras/staa3623](https://doi.org/10.1093/mnras/staa3623)

Michilli, D., Bhardwaj, M., Brar, C., et al. 2023, ApJ, 950, 134, doi: [10.3847/1538-4357/accf89](https://doi.org/10.3847/1538-4357/accf89)

Moe, M., & Di Stefano, R. 2017, ApJS, 230, 15, doi: [10.3847/1538-4365/aa6fb6](https://doi.org/10.3847/1538-4365/aa6fb6)

Moe, M., & Kratter, K. M. 2021, MNRAS, 507, 3593, doi: [10.1093/mnras/stab2328](https://doi.org/10.1093/mnras/stab2328)

Naoz, S. 2016, ARA&A, 54, 441, doi: [10.1146/annurev-astro-081915-023315](https://doi.org/10.1146/annurev-astro-081915-023315)

Naoz, S., Farr, W. M., Lithwick, Y., Rasio, F. A., & Teyssandier, J. 2013a, MNRAS, 431, 2155, doi: [10.1093/mnras/stt302](https://doi.org/10.1093/mnras/stt302)

Naoz, S., Fragos, T., Geller, A., Stephan, A. P., & Rasio, F. A. 2016, ApJL, 822, L24, doi: [10.3847/2041-8205/822/2/L24](https://doi.org/10.3847/2041-8205/822/2/L24)

Naoz, S., Haiman, Z., Quataert, E., & Holzknecht, L. 2025, ApJL, 992, L12, doi: [10.3847/2041-8213/ae0a20](https://doi.org/10.3847/2041-8213/ae0a20)

Naoz, S., Kocsis, B., Loeb, A., & Yunes, N. 2013b, ApJ, 773, 187, doi: [10.1088/0004-637X/773/2/187](https://doi.org/10.1088/0004-637X/773/2/187)

Niu, C. H., Aggarwal, K., Li, D., et al. 2022, Nature, 606, 873, doi: [10.1038/s41586-022-04755-5](https://doi.org/10.1038/s41586-022-04755-5)

Nomoto, K., & Kondo, Y. 1991, ApJL, 367, L19, doi: [10.1086/185922](https://doi.org/10.1086/185922)

Offner, S. S. R., Moe, M., Kratter, K. M., et al. 2023, in Astronomical Society of the Pacific Conference Series, Vol. 534, Protostars and Planets VII, ed. S. Inutsuka, Y. Aikawa, T. Muto, K. Tomida, & M. Tamura, 275, doi: [10.48550/arXiv.2203.10066](https://doi.org/10.48550/arXiv.2203.10066)

Pakmor, R., Kromer, M., Taubenberger, S., et al. 2012, ApJL, 747, L10, doi: [10.1088/2041-8205/747/1/L10](https://doi.org/10.1088/2041-8205/747/1/L10)

Perets, H. B. 2025, arXiv e-prints, arXiv:2504.02939, doi: [10.48550/arXiv.2504.02939](https://doi.org/10.48550/arXiv.2504.02939)

Perrett, K., Sullivan, M., Conley, A., et al. 2012, AJ, 144, 59, doi: [10.1088/0004-6256/144/2/59](https://doi.org/10.1088/0004-6256/144/2/59)

Petroff, E., Hessels, J. W. T., & Lorimer, D. R. 2019, A&A Rv, 27, 4, doi: [10.1007/s00159-019-0116-6](https://doi.org/10.1007/s00159-019-0116-6)

—. 2022, A&A Rv, 30, 2, doi: [10.1007/s00159-022-00139-w](https://doi.org/10.1007/s00159-022-00139-w)

Platts, E., Weltman, A., Walters, A., et al. 2019, PhR, 821, 1, doi: [10.1016/j.physrep.2019.06.003](https://doi.org/10.1016/j.physrep.2019.06.003)

Prochaska, J. X., Macquart, J.-P., McQuinn, M., et al. 2019, Science, 366, 231, doi: [10.1126/science.aay0073](https://doi.org/10.1126/science.aay0073)

Raghavan, D., McAlister, H. A., Henry, T. J., et al. 2010, ApJS, 190, 1, doi: [10.1088/0067-0049/190/1/1](https://doi.org/10.1088/0067-0049/190/1/1)

Rajamuthukumar, A. S., Hamers, A. S., Neunteufel, P., Pakmor, R., & de Mink, S. E. 2023, ApJ, 950, 9, doi: [10.3847/1538-4357/acc86c](https://doi.org/10.3847/1538-4357/acc86c)

Rajamuthukumar, A. S., Korol, V., Stegmann, J., et al. 2025, arXiv e-prints, arXiv:2502.09607, doi: [10.48550/arXiv.2502.09607](https://doi.org/10.48550/arXiv.2502.09607)

Rao, A., Ye, C. S., & Fishbach, M. 2025, ApJL, 979, L12, doi: [10.3847/2041-8213/ad9f2e](https://doi.org/10.3847/2041-8213/ad9f2e)

Ravi, V. 2019, Nature Astronomy, 3, 928, doi: [10.1038/s41550-019-0831-y](https://doi.org/10.1038/s41550-019-0831-y)

Ravi, V., Law, C. J., Li, D., et al. 2022, MNRAS, 513, 982, doi: [10.1093/mnras/stac465](https://doi.org/10.1093/mnras/stac465)

Ruiter, A. J., Belczynski, K., Sim, S. A., et al. 2011, MNRAS, 417, 408, doi: [10.1111/j.1365-2966.2011.19276.x](https://doi.org/10.1111/j.1365-2966.2011.19276.x)

Schwab, J. 2021, ApJ, 906, 53, doi: [10.3847/1538-4357/abc87e](https://doi.org/10.3847/1538-4357/abc87e)

Shah, V., Shin, K., Leung, C., et al. 2025, ApJL, 979, L21, doi: [10.3847/2041-8213/ad9ddc](https://doi.org/10.3847/2041-8213/ad9ddc)

Shappee, B. J., & Thompson, T. A. 2013, ApJ, 766, 64, doi: [10.1088/0004-637X/766/1/64](https://doi.org/10.1088/0004-637X/766/1/64)

Shariat, C., El-Badry, K., & Naoz, S. 2025a, PASP, 137, 094201, doi: [10.1088/1538-3873/adfb30](https://doi.org/10.1088/1538-3873/adfb30)

Shariat, C., El-Badry, K., Naoz, S., Rodriguez, A. C., & van Roestel, J. 2025b, PASP, 137, 074201, doi: [10.1088/1538-3873/add5a1](https://doi.org/10.1088/1538-3873/add5a1)

Shariat, C., Naoz, S., El-Badry, K., et al. 2025c, ApJ, 983, 115, doi: [10.3847/1538-4357/adbf01](https://doi.org/10.3847/1538-4357/adbf01)

—. 2025d, ApJ, 978, 47, doi: [10.3847/1538-4357/ad944a](https://doi.org/10.3847/1538-4357/ad944a)

Shariat, C., Naoz, S., Hansen, B. M. S., et al. 2023, ApJL, 955, L14, doi: [10.3847/2041-8213/acf76b](https://doi.org/10.3847/2041-8213/acf76b)

Sharma, K., Somalwar, J., Law, C., et al. 2023, ApJ, 950, 175, doi: [10.3847/1538-4357/accf1d](https://doi.org/10.3847/1538-4357/accf1d)

Sharma, K., Ravi, V., Connor, L., et al. 2024, Nature, 635, 61, doi: [10.1038/s41586-024-08074-9](https://doi.org/10.1038/s41586-024-08074-9)

Shen, K. J. 2025, ApJ, 982, 6, doi: [10.3847/1538-4357/adb42e](https://doi.org/10.3847/1538-4357/adb42e)

Shen, K. J., & Bildsten, L. 2014, ApJ, 785, 61, doi: [10.1088/0004-637X/785/1/61](https://doi.org/10.1088/0004-637X/785/1/61)

Shen, K. J., Bildsten, L., Kasen, D., & Quataert, E. 2012, ApJ, 748, 35, doi: [10.1088/0004-637X/748/1/35](https://doi.org/10.1088/0004-637X/748/1/35)

Shen, K. J., Blondin, S., Kasen, D., et al. 2021, ApJL, 909, L18, doi: [10.3847/2041-8213/abe69b](https://doi.org/10.3847/2041-8213/abe69b)

Shen, K. J., Kasen, D., Miles, B. J., & Townsley, D. M. 2018, ApJ, 854, 52, doi: [10.3847/1538-4357/aaa8de](https://doi.org/10.3847/1538-4357/aaa8de)

Shen, K. J., & Moore, K. 2014, ApJ, 797, 46, doi: [10.1088/0004-637X/797/1/46](https://doi.org/10.1088/0004-637X/797/1/46)

Shin, K., Masui, K. W., Bhardwaj, M., et al. 2023, ApJ, 944, 105, doi: [10.3847/1538-4357/acaf06](https://doi.org/10.3847/1538-4357/acaf06)

Sridhar, N., Metzger, B. D., Beniamini, P., et al. 2021, ApJ, 917, 13, doi: [10.3847/1538-4357/ac0140](https://doi.org/10.3847/1538-4357/ac0140)

Stegmann, J., Antonini, F., & Moe, M. 2022, MNRAS, 516, 1406, doi: [10.1093/mnras/stac2192](https://doi.org/10.1093/mnras/stac2192)

Stegmann, J., & Klencki, J. 2025, arXiv e-prints, arXiv:2506.09121, doi: [10.48550/arXiv.2506.09121](https://doi.org/10.48550/arXiv.2506.09121)

Stephan, A. P., Naoz, S., Ghez, A. M., et al. 2016, MNRAS, 460, 3494, doi: [10.1093/mnras/stw1220](https://doi.org/10.1093/mnras/stw1220)

Su, Y., & Lai, D. 2022, MNRAS, 510, 4943, doi: [10.1093/mnras/stab3698](https://doi.org/10.1093/mnras/stab3698)

Tang, L., Lin, H.-N., & Li, X. 2023, Chinese Physics C, 47, 085105, doi: [10.1088/1674-1137/acda1c](https://doi.org/10.1088/1674-1137/acda1c)

Tendulkar, S. P., Bassa, C. G., Cordes, J. M., et al. 2017, ApJL, 834, L7, doi: [10.3847/2041-8213/834/2/L7](https://doi.org/10.3847/2041-8213/834/2/L7)

Thompson, T. A. 2011a, ApJ, 741, 82, doi: [10.1088/0004-637X/741/2/82](https://doi.org/10.1088/0004-637X/741/2/82)

—. 2011b, ApJ, 741, 82, doi: [10.1088/0004-637X/741/2/82](https://doi.org/10.1088/0004-637X/741/2/82)

Thornton, D., Stappers, B., Bailes, M., et al. 2013, Science, 341, 53, doi: [10.1126/science.1236789](https://doi.org/10.1126/science.1236789)

Tokovinin, A. 2014a, AJ, 147, 87, doi: [10.1088/0004-6256/147/4/87](https://doi.org/10.1088/0004-6256/147/4/87)

—. 2014b, AJ, 147, 87, doi: [10.1088/0004-6256/147/4/87](https://doi.org/10.1088/0004-6256/147/4/87)

—. 2022, ApJ, 926, 1, doi: [10.3847/1538-4357/ac4584](https://doi.org/10.3847/1538-4357/ac4584)

Toonen, S., Hamers, A., & Portegies Zwart, S. 2016, Computational Astrophysics and Cosmology, 3, 6, doi: [10.1186/s40668-016-0019-0](https://doi.org/10.1186/s40668-016-0019-0)

Toonen, S., Perets, H. B., & Hamers, A. S. 2018, A&A, 610, A22, doi: [10.1051/0004-6361/201731874](https://doi.org/10.1051/0004-6361/201731874)

Toonen, S., Portegies Zwart, S., Hamers, A. S., & Bandopadhyay, D. 2020, A&A, 640, A16, doi: [10.1051/0004-6361/201936835](https://doi.org/10.1051/0004-6361/201936835)

Totani, T. 2013, PASJ, 65, L12, doi: [10.1093/pasj/65.5.L12](https://doi.org/10.1093/pasj/65.5.L12)

Tout, C. A., Wickramasinghe, D. T., Liebert, J., Ferrario, L., & Pringle, J. E. 2008, MNRAS, 387, 897, doi: [10.1111/j.1365-2966.2008.13291.x](https://doi.org/10.1111/j.1365-2966.2008.13291.x)

Usov, V. V. 1992, Nature, 357, 472, doi: [10.1038/357472a0](https://doi.org/10.1038/357472a0)

Vick, M., Lai, D., & Anderson, K. R. 2019, MNRAS, 484, 5645, doi: [10.1093/mnras/stz354](https://doi.org/10.1093/mnras/stz354)

Vick, M., Lai, D., & Fuller, J. 2017, MNRAS, 468, 2296, doi: [10.1093/mnras/stx539](https://doi.org/10.1093/mnras/stx539)

Wang, J.-S., Yang, Y.-P., Wu, X.-F., Dai, Z.-G., & Wang, F.-Y. 2016, ApJL, 822, L7, doi: [10.3847/2041-8205/822/1/L7](https://doi.org/10.3847/2041-8205/822/1/L7)

Will, C. M. 2017, PhRvD, 96, 023017, doi: [10.1103/PhysRevD.96.023017](https://doi.org/10.1103/PhysRevD.96.023017)

—. 2021, PhRvD, 103, 063003, doi: [10.1103/PhysRevD.103.063003](https://doi.org/10.1103/PhysRevD.103.063003)

Xuan, Z., Shariat, C., & Naoz, S. 2025, arXiv e-prints, arXiv:2508.13264, doi: [10.48550/arXiv.2508.13264](https://doi.org/10.48550/arXiv.2508.13264)

Yamasaki, S., Hashimoto, T., Kusakabe, H., & Goto, T. 2025, arXiv e-prints, arXiv:2508.07688, doi: [10.48550/arXiv.2508.07688](https://doi.org/10.48550/arXiv.2508.07688)

Zahn, J. P. 1977, A&A, 57, 383

Zhang, J.-G., Li, Y., Zou, J.-M., et al. 2024, Universe, 10, 207, doi: [10.3390/universe10050207](https://doi.org/10.3390/universe10050207)